Rotational Spectroscopy as a Tool to Study Vibration-Rotation Interaction: Investigations of ^{13}CH$_3$CN and CH$_3^{13}$CN up to $v_8 = 2$ and a Search for $v_8 = 2$ Transitions toward Sagittarius B2(N)

Holger S. P. Müller^{a,*}, Arnaud Belloche^b, Frank Lewen^a, Stephan Schlemmer^a

^{a}*I. Physikalisches Institut, Universität zu Köln, Zülpicher Str. 77, 50937 Köln, Germany*
^{b}*Max-Planck-Institut für Radioastronomie, Auf dem Hügel 69, 53121 Bonn, Germany*

Abstract

Methyl cyanide, CH$_3$CN, is present in diverse regions in space, in particular in the warm parts of star-forming regions where it is a common molecule. Rotational transitions of ^{13}CH$_3$CN and CH$_3^{13}$CN in their $v_8 = 1$ lowest excited vibrational states ($E_{\text{vib}} \approx 520$ K) are quite prominent in Sagittarius B2(N). In order to be able to search for transitions of the next higher vibrational state $v_8 = 2$, we recorded spectra of samples enriched in ^{13}CH$_3$CN and CH$_3^{13}$CN up to $v_8 = 2$ in the 35 to 1091 GHz region and reinvestigated existing spectra of CH$_3$CN in its natural isotopic composition between 1085 and 1200 GHz. Perturbations caused by near-degeneracies in $K = 4$ of $v_8 = 2^0$ and $K = 2$ of $v_8 = 2^{-2}$ yielded accurate information on the energy spacing of 22.93 and 21.79 cm^{-1} between the l-components of ^{13}CH$_3$CN and CH$_3^{13}$CN, respectively. Fermi-type interaction between $K = 13$ and 14 of $v_8 = 1^{-1}$ and $v_8 = 2^{+2}$ probe the energy differences between the two states of both isotopomers. In addition, a $\Delta K \pm 2$, $\Delta l \mp 1$ interaction between the ground vibrational state of ^{13}CH$_3$CN and $v_8 = 1^{+1}$ provides information on their energy spacing. Furthermore, we obtained improved or extended ground state rotational transition frequencies of ^{13}CH$_3^{13}$CN and extensive data for ^{13}CH$_3$C^{15}N and CH$_3^{13}$C^{15}N. Finally, we report the results of our search for transitions of ^{13}CH$_3$CN and CH$_3^{13}$CN in their $v_8 = 2$ states toward Sagittarius B2(N).

Keywords:
absorption spectroscopy, rotational spectroscopy, methyl cyanide, isotopic substitution, vibration-rotation interaction, Fermi resonance, interstellar molecule

1. INTRODUCTION

Methyl cyanide, also known as acrylonitrile or cyanomethane, is important in astrochemistry and in astrophysics. It was detected in Sagittarius (Sgr) A and B more than 50 years ago as one of the first molecules observed by radioastronomical means [1] and the 17th molecule detected in space [2]. Already this first report on CH$_3$CN in space pointed out its potential as a probe into the excitation temperature in these sources because transitions with the same overall rotational quantum number J but different K occur in fairly narrow frequency ranges, but sample very different energies. Methyl cyanide was not only found in high-mass star forming regions, but also in the warm and dense parts of molecular clouds surrounding low-mass protostars [3], in cold, dark molecular clouds [4], in the envelopes of carbon-rich late-type stars [5], in external galaxies [6], in disks around young protostars [7], and in translucent molecular clouds [8].

The molecule is also a trace constituent in Earth's atmosphere, predominantly caused by biomass burning [9, 10]. Concerning the Solar system, it was also found in comets, such as Kohoutek [11], and in the atmosphere of Titan [12].

Methyl cyanide was not only identified in space in its ground vibrational state, but was also detected in its $v_8 = 1$ ($E_{\text{vib}} = 525$ K) [13], $v_8 = 2$ [14], $v_4 = 1$ ($E_{\text{vib}} = 1324$ K) [15], and $v_4 = v_8 = 1$ [16] excited vibrational states, albeit in the last state only tentatively.

Many minor isotopic species of CH$_3$CN were detected in space (here and in the following, unlabeled atoms refer to ^{1}H, ^{12}C, and ^{14}N), which are CH$_3^{13}$CN [17], ^{13}CH$_3$CN [18], CH$_2$DCN [19], CH$_3$C^{15}N [20], and even ^{13}CH$_3^{13}$CN [21] and CHD$_2$CN shortly thereafter [22]. In the case of ^{13}CH$_3$CN and CH$_3^{13}$CN, also transitions in $v_8 = 1$ were identified [15], making transitions in $v_8 = 2$ a next logical target.

Müller et al. [23] provided a comprehensive account on the ground state rotational spectra of CH$_3$CN, all singly substituted isotopologs, as well as ^{13}CH$_3^{13}$CN in natural isotopic composition. In a later study of rotational and rovibrational spectra of CH$_3$CN up to $v_8 = 2$ [24], a resonance between $v = 0$ and $v_8 = 1$ was analyzed in detail for the first time and revealed Fermi-type interactions ($\Delta K = 0$, $\Delta l = \pm 3$) between $v_8 = 1$ and 2 as well as between $v_8 = 2$ and 3 besides numerous other resonances, of which several were not reported previously. A more recent investigation included rotational and rovibrational spectra of CH$_3$CN in $v_4 = 1$ into this analysis with additions or improvements in parts of the lower state data and with the iden-

*Corresponding author.
Email address: hspm@ph1.uni-koeln.de (Holger S. P. Müller)

tification of further resonances, some identified newly [16].

Müller et al. [25] presented extensive analyses of $^{13}CH_3CN$, $CH_3^{13}CN$, and $CH_3C^{15}N$ in their $v_8 = 1$ states using a sample in natural isotopic composition. Even though the accessed K levels did not reach high enough to cover the region of stronger interactions between $v_8 = 1$ and 2, it was still necessary to account for these interactions by estimating $v_8 = 2$ parameters as well as some interaction parameters based on those of the main isotopic species. These reports are testament to methyl cyanide also being of great interest for basic science, in particular spectroscopy, and as a test case for quantum chemistry.

As the $v_8 = 1$ lines of $^{13}CH_3CN$ and $CH_3^{13}CN$ in natural isotopic composition were already too weak prior to reaching K level experiencing the strongest $v_8 = 1/2$ perturbations, our present investigation is based on new spectral recordings between 35 and 1091 GHz employing samples enriched in $^{13}CH_3CN$ and $CH_3^{13}CN$, respectively. We did study these isotopomers not only in their $v_8 = 2$ states, but also in $v = 0$ and $v_8 = 1$. As added boni, we extended the data set of $^{13}CH_3^{13}CN$ from the previous study [23] and obtained extensive line lists for $^{13}CH_3C^{15}N$ and $CH_3^{13}C^{15}N$, for which only limited data up to 72 GHz were available thus far [26].

The remainder of the paper is organized as follows. Information on the measurements is given in Section 2, Section 3 provides clues on the rotational and vibrational spectroscopy of CH_3CN isotopologs relevant to this study, and Section 4 reveals how the rotational spectra were calculated and fit. The results of our laboratory measurements are described in Section 5, Section 6 discusses these results, Section 7 presents the astronomical results, and conclusions are given in Section 8.

2. EXPERIMENTAL DETAILS

Measurements at the Universität zu Köln were carried out between 35 and 1091 GHz applying three slightly different spectrometer setups. All utilize glass cells of different lengths and 100 mm inner diameter kept at room temperature. All new measurements were carried out employing methyl cyanide samples enriched in $^{13}CH_3CN$ or $CH_3^{13}CN$ (Sigma-Aldrich Chemie GmbH) with 99% ^{13}C at the respective position; there was no indication of ^{13}C enrichment at the other C atom. Sample pressures were in the range of 0.5 to 1.0 Pa in most cases; pressures of 0.1 Pa or less were applied for measurements of the low K (≤ 12) transitions in the ground vibrational states, whereas pressures of 2.5 Pa or slightly higher were chosen for very weak lines. No unexpected or unusually high safety hazards were encountered in the course of our investigations. In order to minimize any risk, it is strongly recommended to follow safety precautions listed in the safety data sheets and use small quantities, about 1 g at most, preferably less, at a time.

An Agilent E8257D synthesizer at fundamental frequencies was used for measurements between 35 and 56 GHz, while this synthesizer together with a VDI frequency tripler was employed between 71 and 111 GHz. The measurements were done in two connected 7 m long glass cells in a single path arrangement. This setup is a modification of the one employed in ref. 27.
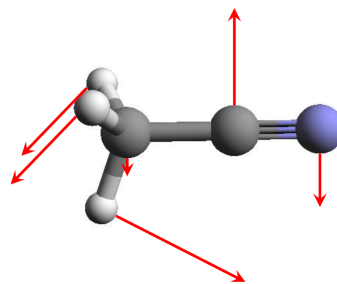

Figure 1: Model of the methyl cyanide molecule with the v_8 displacement vectors. The C atoms are shown in gray, the H atoms in light gray, and the N atom in blue. The a-axis is along the CCN atoms and is also the symmetry axis. The lengths of the v_8 displacement vectors are exaggerated.

Various active and passive frequency multipliers from the VDI starter kit driven by Rohde & Schwarz SMF 100A or Keysight E8257D synthesizers were used for higher frequencies. A 5 m long double path cell served for measurements in the 160 to 252 GHz region. The spectrometer was described in detail earlier [28]. The glass cells at these lower frequencies were equipped with Teflon windows and Schottky-diode detectors.

Measurements between 355 and 1091 GHz were carried out in a 5 m long single path cell sealed with HDPE windows. A closed-cycle liquid He cooled bolometer (QMC Instruments Ltd) served as detector. Frequency modulation was applied throughout; the demodulation at $2f$ causes the lines to appear similar to a second derivative of a Gaussian. Further information on this spectrometer system is available elsewhere [29].

Part of the spectral recordings were broader scans, frequently covering about one vibrational state of one isotopolog with integration times adjusted to achieve very good signal-to-noise ratios (S/N) for fairly weak lines. Very weak lines were recorded individually with integration times adjusted to reach at a least good S/N in each case. In addition, some of the stronger lines were recorded in single line scans.

We also inspected broad frequency scans of CH_3CN in natural isotopic composition covering $1083-1200$ GHz and taken much earlier [23] with the JPL cascaded multiplier spectrometer [30]. These scans have especially good S/N among the JPL scans and are mostly higher in frequency than recordings taken in Cologne. A multiplier chain source is passed through a one to two-meter path length flow cell and is detected by a silicon bolometer cooled to near 1.7 K for these recordings. The cell is filled with a steady flow of reagent grade acetonitrile. Pressure and modulation are optimized to yield good S/N with narrow lineshapes. The S/N was optimized for a higher K ground state transition ($K = 12$), such that the lower K transitions exhibit saturated line profiles. This way, a better dynamic range was obtained for lines of the rare isotopologs and for highly excited vibrational satellites.
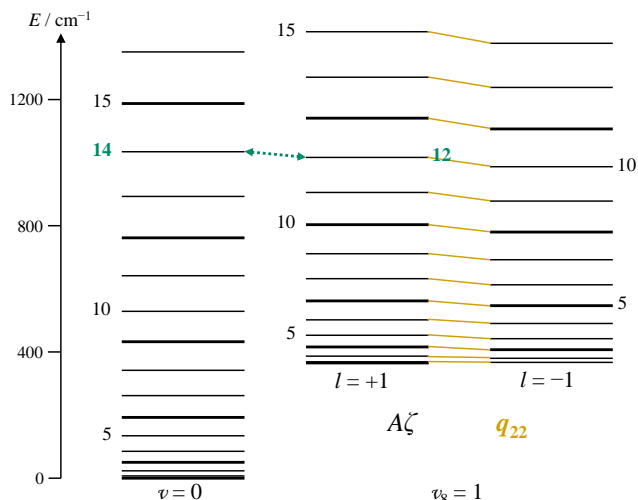
Figure 2: $J = K$ energy levels of methyl cyanide $v = 0$ on the left and the doubly degenerate $v_8 = 1$ on the right; with the latter separated into their $l = +1$ and $l = -1$ substates. Levels with $k - l \equiv 0$ mod 3 have A symmetry while all others have E symmetry. A symmetry levels are shown with thicker lines. The Coriolis interaction between the two $l = \pm 1$ substates of $v_8 = 1$ with the lowest order parameter $A\zeta$ shifts $l = +1$ down in energy and $l = -1$ up in energy, causing levels in $v_8 = 1$ having the same $K - l$ to be close in energy, facilitating q_{22} interaction. Note the proximity of $K = 12$ of $v_8 = 1^{+1}$ to $K = 14$ of $v = 0$. The $K = 0$, 1, and 2 levels of $v_8 = 1^{+1}$ are so close in energy that their lines in the figure appear as one.

Figure 3: Low-K energy level structure of the triply degenerate $v_8 = 2$ of $^{13}CH_3CN$ on the left and of $CH_3^{13}CN$ on the right, separated into their $l = 0$, $l = -2$, and $l = +2$ substates. Here, the hypothetical $J = 0$ level energies are shown. The Coriolis interaction between the two $l = \pm 2$ substates of $v_8 = 2$ shifts the $l = +2$ levels down in energy and the $l = -2$ levels up in energy, causing levels having the same $K - l$ to be close in energy, as indicated by magenta lines, facilitating again q_{22} interaction, similer to $v_8 = 1$. Note that $K = 4$ of $l = 0$ and $K = 2$ of $l = -2$ are very close in energy with the former being slightly lower than the latter in the case of $^{13}CH_3CN$ whereas it is opposite in the case of $CH_3^{13}CN$. Note also that for $l = +2$ $K = 1$, 2, and 3 are lower in energy than $K = 0$.

3. SPECTROSCOPIC PROPERTIES OF CH$_3$CN

Methyl cyanide is a C_{3v} symmetric top molecule of the prolate type with $A \gg B$ as the light H atoms are the only ones not on the symmetry axis of CH$_3$CN, see Figure 1. The general selection rules are $\Delta k - \Delta l \equiv 0$ mod 3, with k being the product of K and the sign of l for $l \neq 0$ and with an unsigned k indicating an $l = 0$ (sub-) state.

The CH$_3$CN ground state dipole moment of 3.92197 (13) D [31] leads to very strong transitions, which obey $\Delta K = 0$ selection rules. The Boltzmann peak at 300 K is near 600 GHz at J values slightly above 30, and the intensities near 1090 GHz are only 15% of the peak intensities. $\Delta K = 3$ transitions gain intensity through centrifugal distortion effects, but are usually too weak to be observed. Therefore, the purely axial parameters A (or $A - B$), D_K, etc. cannot be determined by rotational spectroscopy, unless perturbations are present. Rovibrational spectroscopy yields, strictly speaking, the differences ΔA (or $\Delta(A - B)$), ΔD_K, etc. from single state analyses. Thus, the ground state axial parameters cannot be determined from such fits either. In the case of CH$_3$CN, they were determined through analyses of three IR bands involving two doubly degenerate vibrational modes, ν_8, $\nu_7 + \nu_8$, and $\nu_7 + \nu_8 - \nu_8$ [32], and were improved through perturbations [24, 16]. The large value of A, ~5.27 cm^{-1}, leads to a rapid increase in the ground state rotational energy with K, as shown in Figure 2 for the $J = K$ lowest rotational levels.

Substitution of an atom on the C_{3v} symmetry axis does not affect the equilibrium A rotational parameter in the Bo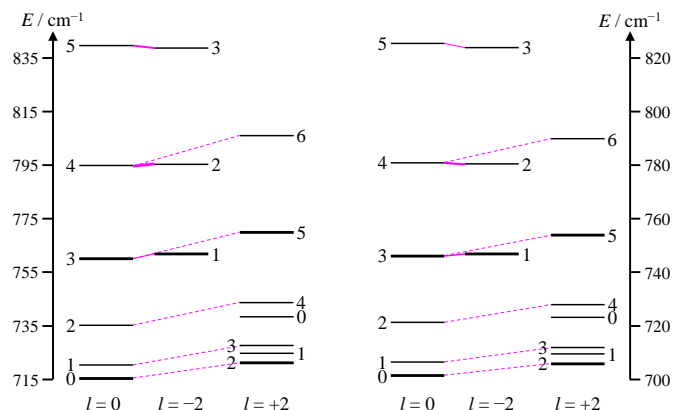rn-Oppenheimer approximation. Therefore, it was assumed that the A_0 ground state rotational parameters do not change upon such substitution either. While this assumption probably does not hold strictly, deviations are most likely small.

The lowest CH$_3$CN vibration is the doubly degenerate ν_8 at 365.024 cm^{-1} [24, 16]. It is commonly described as the CCN bending mode, but the displacement vectors in Figure 1 suggest that it is better described as a combination of the CCN bending mode with additional CH$_3$ wagging character. The displacement vectors are from a B3LYP [33, 34] quantum chemical calculation with the aug-cc-pVTZ basis set [35] employing Gaussian 03 [36]. The displacement vectors were lengthend to make the one of the methyl-C better visible. Strong Coriolis interaction between the l components is frequently observed in low-lying degenerate bending modes. The Coriolis parameter ζ in $\nu_8 = 1$ of CH$_3$CN is 0.8775, close to the limiting case of 1. The K levels with $l = +1$ are pushed down in energy, and those with $l = -1$ are pushed up with the result that levels with the same $K - l$ are close in energy (Figure 2). These levels have the same symmetry and can thus repel each other through q_{22} ($\Delta k = \Delta l = \pm 2$) interaction.

There are three l components in the case of $v_8 = 2$ with $l = 0$ and $l = \pm 2$ with origins at 716.750 and 739.148 cm^{-1}, respectively, for CH$_3$CN (Figure 3). The effective strength of the Coriolis interaction between the $l = +2$ and $l = -2$ levels is two times that between the $l = \pm 1$ components in $v_8 = 1$, causing levels with the same $K - l$ for all three l components to be close in energies to a different degree, as indicated by the magenta lines in Figure 3 for low-K values.

The three H atoms are equivalent in CH$_3$CN as well as in isotopologs with substitutions on the C_{3v} axis. This leads to levels with $k - l \equiv 0$ mod 3 having A symmetry and all other levels having E symmetry. A level transitions, except those with

3

$K = 0$ of (sub-) states with $l \equiv 0$ mod 3, are twice as strong as E levels with about the same energy. However, these A levels may in theory be split further into A_1 and A_2 (or A_+ and A_-) levels. Such splitting was not resolved for CH_3CN and its ^{13}C isotopologs in $k = 3$ of $v = 0$ and even much less so for higher k. However, $k = +1$ of $v_8 = 1$ is widely split by the q_{22} interaction the two lines are often designated as $k = l = -1$ and $k = l = +1$, respectively; the splitting of $k = -2$ of $v_8 = 1$ is usually not resolved, and levels with higher K even less so. In the case of $v_8 = 2$, the splitting in $k = +2$ by the q_{22} interaction is frequently resolvable, as can be seen in Figure 4 close to the upper frequency edge of each trace. The splitting in other k levels is by far too small to be resolved.

4. CALCULATION AND FITTING OF THE SPECTRA

The calculation of the $^{13}CH_3CN$ and $CH_3{}^{13}CN$ rotational spectra and the fitting of the data were carried out with Pickett's SPCAT and SPFIT programs [37]. The programs were written as general purpose programs to be capable of treating asymmetric top rotors with spins and with vibration-rotation interaction. They have evolved considerably with time because of added features, in particular special considerations for symmetric top or linear molecules or for higher symmetry cases [38, 39, 40].

We evaluated rotational, centrifugal, and hyperfine structure (HFS) parameters of the ground state as common for all vibrational states. Some of the data were measured or reported with partial or fully resolved HFS, but the majority of the data were not affected by HFS. Therefore, all states were defined twice, with and without HFS. The HFS parameter $eqQ\eta$, also designated as eQq_2, may require some explanation. It is the nuclear quadrupole analog of the l-type doubling parameter q [41, 42]. It corresponds to an off-diagonal $\chi_{bb} - \chi_{cc}$ in an asymmetric top molecule and may be better known as eQq_2 from the rotational spectroscopy of π radicals. Vibrational changes $\Delta X = X_i - X_0$ to the ground vibrational state were fit for excited vibrational states, where X represents a parameter and X_i and X_0 represent the parameter in excited and ground vibrational states, respectively. This is very similar to several early studies on CH_3CN [43, 44], identical to our previous reports [24, 25, 16], and rather convenient because vibrational corrections ΔX are usually small with respect to X, especially in the case of low order parameters. Moreover, this procedure offers the opportunity to constrain vibrational corrections, for example the distortion parameters of $v_8 = 2$ to twice those of $v_8 = 1$, thus reducing the amount of independent spectroscopic parameters further. New parameters in the fit were chosen carefully by searching for the parameter that reduces the rms error of the fit the most. We tried to assess if the value of a new parameter is reasonable in the context of related parameters and tried to omit or constrain parameters whose values changed considerably in a fit or had relatively large uncertainties. Care was also taken that a new parameter is reasonable with respect to quantum numbers of newly added transition frequencies or that it can account for systematic residuals.

The spectroscopic parameters used in the present analyses are standard symmetric rotor parameters defined and designated in a systematic way. The designation of the interaction parameters in particular may differ considerably with respect to other publications, and there may be small changes in the details of their definitions. Therefore, we give a summary of the interaction parameters in the following. Fermi and other anharmonic interaction parameters are designated with a plain F and are used in the same way irrespective of a $\Delta l = 0$ or $\Delta l = 3$ interaction because the SPFIT and SPCAT programs use only $l = 0$ and ± 1. The parameters G_b and F_{ac} are first and second order Coriolis-type parameters, respectively, of b-symmetry, i.e., they are coefficients of iJ_b and $(J_aJ_c + J_cJ_a)/2$, respectively. The parameters G_a and F_{bc} are defined equivalently. The interacting states are given in parentheses separarated by a comma; the degree of excitation of a fundamental and the l quantum number are given as superscripts separated by a comma if necessary. Rotational corrections to these three types of parameters are designated with J and K subscripts, respectively, as is usually the case. There may also be $\Delta k = \Delta l = \pm 2$ corrections (i.e. $J_+^2 + J_-^2$; where $J_\pm = J_a \pm iJ_b$) to these parameters; they are indicated by a subscript 2. Higher order corrections with $\Delta k = \Delta l = \pm 4$ etc. are defined and indicated equivalently. Additional aspects relevant to the spectroscopy of CH_3CN were detailed earlier [24, 25, 16]. Further, and more general information on SPFIT and SPCAT is available in [45] and in [46] and in the Fitting Spectra section[47] of the Cologne Database for Molecular Spectroscopy, CDMS [48, 49, 50]. It is worthwhile mentioning that there is only one $K = 0$ in states having $l = \pm 1$ or $l = \pm 2$, and the assignment to the respective l component is arbitrary in theory. In SPCAT and SPFIT, $K = 0$ is associated with $l = -1$ and with $l = +2$.

Initial spectroscopic parameters for $^{13}CH_3CN$ and $CH_3{}^{13}CN$ $v_8 \leq 2$ were evaluated by taking the respective parameters from our $v_8 = 1$ study of isotopic methyl cyanide [25]. Estimated parameters were added or adjusted based on our latest results on CH_3CN [16]. Parameters of $^{13}CH_3CN$ and $CH_3{}^{13}CN$ determined in the $v = 0$ investigation [23] and in the $v_8 = 1$ study [25] were then fit to the respective $v_8 \leq 1$ data.

5. LABORATORY SPECTROSCOPIC RESULTS

In the following, we describe our results obtained in the course of the present investigation. Each part detailing observations starts with a brief description of the previous data available and those used in this study. Section 5.1 deals with the results for $v_8 = 2$ of $^{13}CH_3CN$ and $CH_3{}^{13}CN$, the corresponding results for $v_8 = 1$ are given in Section 5.2, and the ones for the ground vibrational states in Section 5.3. Details on the combined fits of these three vibrational states of both isotopomers are presented in Section 5.4, and Section 5.5 contains the results obtained for three doubly substituted CH_3CN isotopologs.

5.1. $v_8 = 2$ States of $^{13}CH_3CN$ and $CH_3{}^{13}CN$

The only published $v_8 = 2$ transition frequencies of $^{13}CH_3CN$ and $CH_3{}^{13}CN$ were reported, to the best of our knowledge, in ref. 51. These comprise $J = 1 - 0$ to $3 - 2$ up to 55.5 GHz. After fitting these data, $J = 6 - 5$ transition frequencies from earlier recordings in natural isotopic composition [24, 25] around
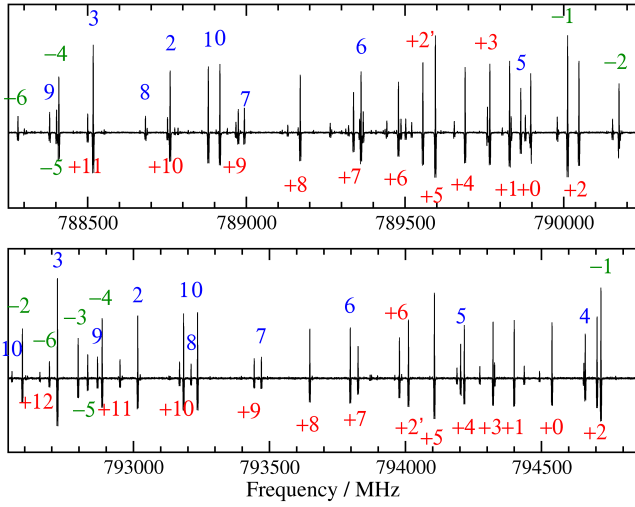
Figure 4: Section of the submillimeter spectrum of $^{13}CH_3CN$ in the region of the $v_8 = 2$ $J = 44 - 43$ transitions on the upper trace and of $CH_3^{13}CN$ in the region of $v_8 = 2$ $J = 43 - 42$ on the lower trace. The k values of the different l substates are indicated centered above or below the line, for $l = 0$ without a sign, and in different colors; see Section 3 for the definition of k. The patterns of both isotopomers are quite similar, in particular with the decrease in frequency for increasing k in the case of $l = +2$ (red); two lines appear for $k = +2$ because the respective levels are split by q_{22} interaction, see also Section 3. Note, however, that $k = -2$ (in green) occurs at the high frequency edge on the upper trace, whereas it occurs near the low frequency part on the lower trace. Similarly, $k = 4$ (in blue) is near the high frequency edge on the lower trace, whereas it is slightly off the low frequency edge of the upper trace. This is caused by the near-degeneracy of $k = -2$ and $k = 4$ together with the q_{22} interaction, see also Figure 3.
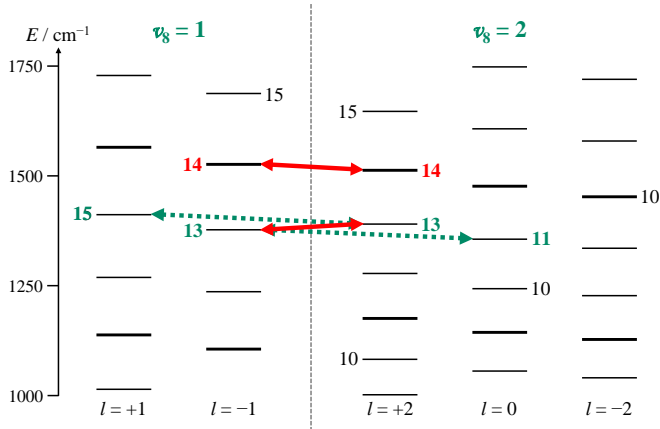

Figure 5: Section of the $J = K$ energy levels of $^{13}CH_3CN$ $v_8 = 1$ on the left and $v_8 = 2$ on the right displaying the K levels around their interactions. Levels having the same $K - l$ in $v_8 = 1$ are close in energy, and this occurs also within $v_8 = 2$. Energy levels with $K = 13$ or 14 in $v_8 = 1^{-1}$ and in $v_8 = 2^{+2}$ are close in energy, giving rise to Fermi-type interaction ($\Delta K = \Delta J = 0$, $\Delta l = \pm 3$). In addition, $K = 13$ of $v_8 = 1^{-1}$ and $K = 11$ of $v_8 = 2^0$ get close in energy, as do $K = 15$ of $v_8 = 1^{+1}$ and $K = 13$ of $v_8 = 2^{+2}$; see also Section 5.1.

107.8 GHz and around 110.9 GHz, respectively, could be assigned. These data were omitted later because of new and more accurate measurements.

After fitting of these data, assignments above 788 and 774 GHz were made in spectral recordings of samples enriched in $^{13}CH_3CN$ and $CH_3^{13}CN$, respectively. Large fractions of two low J transitions of these recordings, $J = 44 - 43$ for $^{13}CH_3CN$ and $43 - 42$ for $CH_3^{13}CN$, are shown in Figure 4 with the k values indicated above or below each line. The patterns of both isotopomers exhibit similarities that are most obvious for the $l = +2$ components in red for which the frequencies decrease with increasing k. The $k = +2$ lines only seem to be displaced because of their splitting caused by the q_{22} interaction, the average positions are between $k = +1$ and $+3$. The $l = 0$ patterns in blue are more irregular, but some resemblance to each other is noticeable. However, there are pronounced differences also. Whereas $k = 4$ of $CH_3^{13}CN$ in the lower trace occurs near the high frequency edge, it is below the low frequency edge of the upper trace in the case of $^{13}CH_3CN$. The $k = -2$ lines in green mirror this appearance, as it is at the upper frequency edge in the upper trace for $^{13}CH_3CN$, whereas it is near the lower frequency edge in the lower trace for $CH_3^{13}CN$. As one can see in Figure 3, $k = 4$ and $k = -2$ are very close in energy. However, $k = -2$ is ~0.36 cm^{-1} higher than $k = 4$ for low-J values of $^{13}CH_3CN$, whereas it is ~0.41 cm^{-1} lower in the case of $CH_3^{13}CN$. The q_{22} interaction and the proximity of these levels cause them to repel each other, shifting the upper level up in energy and the lower level down. This particular interaction, and also the less pronounced ones for other, in particular low k values of $l = 0$ and $l = -2$, cause irregularities in the k line patterns in the spectrum and permit accurate evaluations of the $l = 0$ and $l = \pm 2$ energy differences.

After having established the energy differences between the l components of $v_8 = 2$ for both ^{13}C containing isotopomers, assignments of transitions in broader frequency regions were straightforward for most k up to fairly high values. These broad scans covered many J up to near the upper frequency limit near 1090 GHz and reached $J = 60 - 59$ and $59 - 58$ for $^{13}CH_3CN$ and $CH_3^{13}CN$, respectively.

As expected, deviations from the calculations were somewhat larger at higher K in the $l = +2$ substate, mainly because of a Fermi-type resonance with $v_8 = 1^{-1}$ at $K = 13$ and 14, as can be seen in Figure 5. The energy levels of $^{13}CH_3CN$ and $CH_3^{13}CN$ are very similar mainly because of the very small isotopic v_8 shift of ~0.25 cm^{-1}, whereas the shift is nearly 8 cm^{-1} for $CH_3^{13}CN$. This resonance had to be considered already in our investigation of $v_8 = 1$ of $^{13}CH_3CN$ and $CH_3^{13}CN$ in natural isotopic composition [25] even though k values only reached -11 and -10, respectively. The energies of $K = 13$ in low J of $v_8 = 1^{-1}$ are ~15 cm^{-1} lower than $K = 13$ in $v_8 = 2^{+2}$ in the case of $^{13}CH_3CN$, and the energy differences increase for higher J. The energies of $K = 14$ in low J of $v_8 = 1^{-1}$ are ~13 cm^{-1} lower than $K = 14$ in $v_8 = 2^{+2}$, but the energy differences decrease to higher J, but are still ~7 cm^{-1} at $J = 70$. The situation is qualitatively similar for $CH_3^{13}CN$, but the energy difference is only ~5 cm^{-1} at low J for $K = 13$, increasing to ~11 cm^{-1} at $J = 70$, whereas it is nearly ~24 cm^{-1} at low J for $K = 14$,
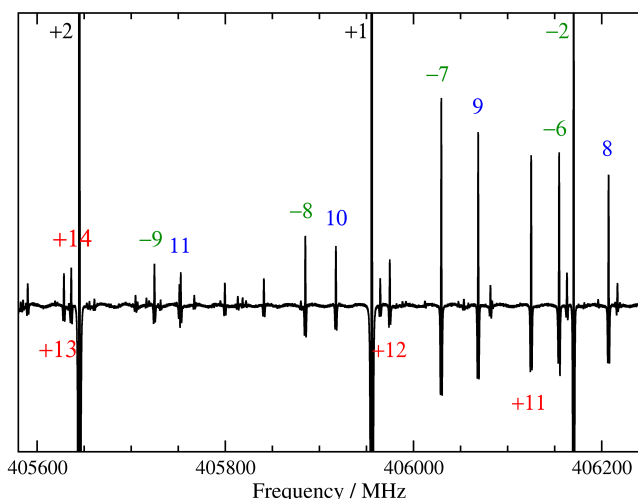
Figure 6: Section of the submillimeter spectrum of CH$_3$^{13}CN in the region of $v_8 = 2$ $J = 22 - 21$ displaying the effect of the $\Delta l = \pm 3$ Fermi-type resonance. Transitions with $k = +11$, 9, and -7 occur at successively lower frequencies, as do $k = +12$, 10, and -8 lower still. However, $k = +13$ is shifted down in frequency by more than 150 MHz, whereas $k = +14$ is shifted up to a frequency slightly higher than $k = +13$. Two clipped lines labeled with $k = +2$ and $+1$ belong to $v_8 = 1$ of CH$_3$^{13}CN.

decreasing to still ~17 cm^{-1} at $J = 70$. The effect of this resonance can be seen in Figure 6. Lines with the same values of $K - l$ occur at similar frequencies at these higher K values with the $l = +2$ line being higher than the $l = 0$ line, which in turn is higher than the $l = -2$ line. This holds for $k = +11$, 9, and -7 as well as for $k = +12$, 10, and -8. However, $k = +13$ is shifted down well below $k = -9$, and $k = +14$ is shifted up to slightly above $k = +13$.

As indicated in Figure 5, there are two additional resonances between $v_8 = 2$ and $v_8 = 1$; one is between $k = 11$ and $k = -13$, with an avoided crossing between $J = 68$ and 69 for ^{13}CH$_3$CN, slightly too high in J to be covered in the present investigation, and the other is between $k = +13$ and $k = +15$ with an avoided crossing between $J = 59$ and 60 for the same isotopolog. Transitions involving these J values as well as many lower ones and up to $J = 61$ are in our data set for one or both k. The perturbations exceed 100 MHz for the most affected transitions and are still larger than 10 MHz in transitions with $J'' \geq 54$ in our data set. Both avoided crossings also occur for the main isotopolog, but at slightly lower J, at $J = 60$ instead of 68/69 in the first case and at $J = 52/53$ instead of 59/60 in the second case [24]. No avoided crossing occurs in the J range covered for CH$_3$^{13}CN as the energy differences still exceed 6 cm^{-1} at $J = 70$ for both resonances. The perturbed lines are shifted by less than 1 MHz for this isotopolog.

Low-K lines, in particular those exhibiting the strongest q_{22} perturbations, as well as high-K lines of the $l = +2$ substate were recorded individually for the transitions above 770 GHz that were not covered by broad scans. At lower frequencies, $J = 2 - 1$ to $6 - 5$ were recorded, which exhibit HFS split transitions almost throughout. In addition, transitions of some J were recorded between ~160 and ~630 GHz.

After having completed the analyses of the present spectral recordings, we inspected spectral recordings of methyl cyanide in natural isotopic composition covering most of the 1083 to 1200 GHz region that were taken at JPL much earlier. We expected at least some lines to have sufficiently good S/N because we had made ^{13}CH$_3$^{13}CN assignments in that region [23]. The strongest lines of $v_8 = 2$ of both isotopomers exhibited quite good S/N between 1085 and 1148 GHz; the lines were too weak at still higher frequencies.

Assigned transitions extend to $k = +15$ for both ^{13}CH$_3$CN and CH$_3$^{13}CN, fitting reasonably well for most of the former, and less so for the latter isotopomer. Poorly fitting lines appearing not to be blended where kept in the fit, but with sufficient MHz values added to the uncertainties, essentially weighting out these lines. Lines turning out to be perturbed, may be weighted in if the perturbation will have been resolved. Very small numbers of assignments of $k = +16$ and $+17$ exist for both isotopomers, but none of them fit well at present.

In the case of the $l = 0$ substate, assigned transitions reach $K = 12$ plus two $K = 13$ lines in the case of ^{13}CH$_3$CN, with lines fitting well for the most part up to $K = 7$ for both isotopomers. All but one transitions with $K = 9$ fit well for CH$_3$^{13}CN. The deviations for $K \geq 10$ are probably caused for the most part by a Fermi-type resonance with $v_8 = 3^{+3}$ which were calculated to be strongest at $K = 15$ for the main isotopolog [24]. Transitions with $K = 8$ may be perturbed by $K = 5$ of $v_4 = 1$, for which an avoided crossing occurs at $J = 57$ for CH$_3$CN [16]. The small and regular deviations in $K = 9$ of ^{13}CH$_3$CN are not easily explained at present. Untangling of these perturbations is beyond the scope of the present investigation, as it would probably not suffice to estimate spectroscopic parameters for $v_4 = 1$, $v_7 = 1$, and $v_8 = 3$ from values of the main isotopolog [16]. Instead, it is probably necessary to include $v_7 = 1$ and $v_8 = 3$ data of the main isotopic species and redetermine its parameters prior to a meaningful estimation of parameters of the singly substituted ^{13}C isotopomers. In addition, we may have to include at least some experimental data for the three higher vibrational states of the ^{13}C isotopomers to adjust B and possibly some additional low order parameters along with some of the multitude of interaction parameters. We point out that vibrational energies of $v_4 = 1$ and $v_7 = 1$ of methyl cyanide isotopologs are fairly well known from low-resolution IR measurements [52].

We assigned up to $K = 10$ in the $l = -2$ substate plus one $K = 11$ line for ^{13}CH$_3$CN. The lines fit well up to $K = 5$; $K = 6$ interacts with $K = 5$ of $v_4 = 1$, this may also apply to the next higher K. Effects of a Fermi-type resonance between $v_8 = 2^{-2}$ and $v_8 = 3^{+1}$, that is strongest at $K = 12$ and 13, may already affect $K = 7$ of $v_8 = 2^{-2}$, almost certainly $K = 8$ and higher. The line lists of both isotopomers are available as Supporting Information and have also been deposited in the CDMS as detailed in the Data Availability Statement.

5.2. $v_8 = 1$ States of ^{13}CH$_3$CN and CH$_3$^{13}CN

The previous $v_8 = 1$ transition frequencies of ^{13}CH$_3$CN and CH$_3$^{13}CN were taken from Ref 25 and originated entirely from that work. Earlier limited low frequency data [51] were already
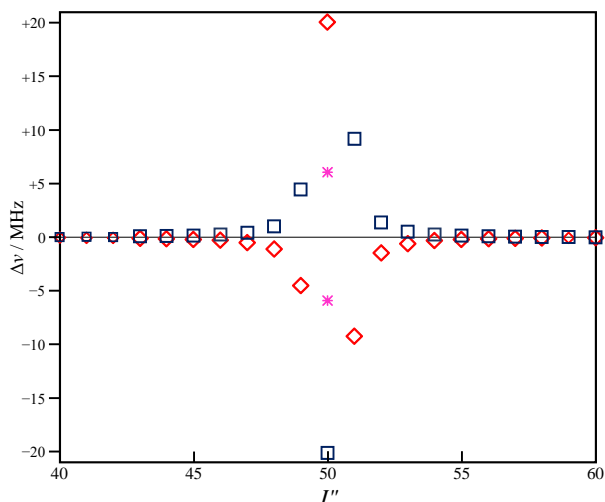
Figure 7: Perturbation plot of $^{13}CH_3CN$. Differences $\Delta\nu$ between the $J' - J''$ transition frequencies calculated from the final spectroscopic parameters and those calculated with the interaction parameter $F_2(0, 8^{\pm1})$ set to zero are shown for $v = 0$ $K = 14$ (blue squares) and $v_8 = 1^{+1}$ $K = 12$ (red diamonds). Larger symbols indicate transitions in the final fit. The very weak cross ladder transitions (magenta) were not observed.

Figure 8: Reduced energy plot of $^{13}CH_3CN$ in the region of $v = 0$ $K = 14$ (blue squares) and $v_8 = 1^{+1}$ $K = 12$ (red diamonds) displaying the resonant interaction at $J = 51$. Larger symbols indicate levels that have been accessed by experimental transitions in the final fit. This interaction probes the $v_8 = 1$ vibrational energy as 364.77 cm^{-1}.

omitted in that work because then new $J = 3 - 2$ data were obtained with much higher accuracies. The transition frequencies with HFS splitting involve $J = 3 - 2$ and $6 - 5$ for both isotopomers and $5 - 4$ for $CH_3^{13}CN$.

The new measurements cover many k of several J values as well as recordings of individual lines in particular at higher k values, similar to the $v_8 = 2$ recordings. The k values reached +16, +17, −15, and −16 in several cases and the next two pairs of k only in 0 to 2 cases. Emphasis was put on measuring transitions with k involved in $v_8 = 2$ interactions.

While the proximity of $k = 14$ in $v = 0$ and $k = +12$ in $v_8 = 1$ was known, see Figure 2, it appeared initially that the energy differences would be too large for both ^{13}C isotopomers to access a level crossing. However, some regularly increasing deviations appeared in $k = +12$ starting at $J = 44 - 43$ near 785 GHz in the case of $^{13}CH_3CN$. Inspection of the energy file revealed a level crossing to occur at $J = 51$. The deviations in $k = 14$ of $v = 0$ mirrored these deviations; the largest ones were 20 MHz for the $J = 51 - 50$ transitions, as can be seen in Figure 7. Figure 8 displays part of the reduced energy plot involving these two k values, demonstrating that they only get very close in energy near J of 51. The level crossing is at $J = 42/43$ for CH_3CN [24], whereas it is calculated to be at $J = 91/92$ for $CH_3^{13}CN$, well outside the covered J range and probably much too weak to be observable, as the Boltzmann peak at 300 K is at $J = 32 - 31$.

5.3. $v = 0$ States of $^{13}CH_3CN$ and $CH_3^{13}CN$

The previous $v = 0$ transition frequencies of $^{13}CH_3CN$ and $CH_3^{13}CN$ were taken from ref. 23 with then new data between 312 and 1193 GHz. The line lists contained earlier data from ref. 53 with frequencies for the hyperfine split $J = 1 - 0$ transitions along with unsplit transition frequencies between 294
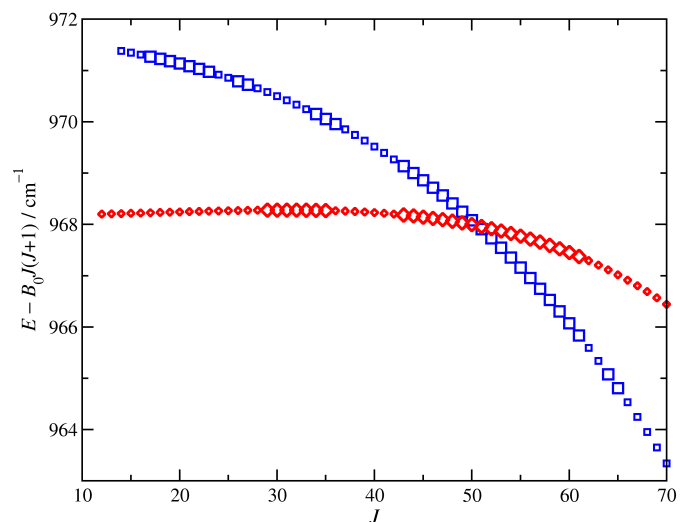
and 608 GHz. Almost all of these data were retained, except a few transition frequencies of $CH_3^{13}CN$ near 440 GHz. Also included were some millimeter data [54] which were eventually omitted in the present work because of newly recorded, much more accurate data at similar frequencies. Finally, accurate transition frequencies of the $J = 2 - 1$ transition of $CH_3^{13}CN$ [55] were also included previously and are retained in the present work.

The new measurements from this study cover transitions with HFS splitting between 35 and 111 GHz ($J = 2 - 1$ to $6 - 5$) with data of the $J = 4 - 3$ transition of $^{13}CH_3CN$ near 71.46 GHz taken from earlier recordings of a sample in natural isotopic composition because of its better quality. Transitions without HFS splitting were recorded between 355 and 1087 GHz, reaching $J = 61 - 60$ and $59 - 58$ for $^{13}CH_3CN$ and $CH_3^{13}CN$, respectively, covering a fair fraction of J in this region, in particular at higher frequencies. The K range was covered as completely as possible, reaching $K = 21$ two times in the case of $CH_3^{13}CN$ and $K = 19$ two times for $^{13}CH_3CN$, in both cases for two J values with frequencies slightly above 600 GHz. Transitions with $K = 14$ were recorded later for $^{13}CH_3CN$ between $J = 54 - 53$ to $61 - 60$ because of the resonance of $v = 0$ and $v_8 = 1$ as mentioned in the previous Section 5.2.

5.4. Fitting of the $^{13}CH_3CN$ and $CH_3^{13}CN$ Data

The $v_8 \leq 2$ data of each singly ^{13}C substituted isotopomer were fit together employing Pickett's SPFIT program [37], as done in earlier reports on the main isotopic species [24, 16]. The equilibrium A value does not change upon substituting one of the atoms on the C_{3v} axis; therefore, we assumed that A in $v = 0$ and the ΔA values of excited vibrational (sub-) states do not change either for such substitutions. This is the same procedure as in our $v_8 = 1$ study of singly substitued methyl

cyanide isotopologs [25] for $v = 0$, but slightly different for the excited states, as we assumed earlier $\Delta(A - B)$ to be the same for a given vibrational (sub-) state upon subsition on the C_{3v} axis. Either assumption is probably reasonable, but unlikely to hold strictly; deviations of order of 1 or a few MHz are deemed to be possible. The isotopic ratios of higher order spectroscopic parameters were estimated to scale with appropriate powers of B, as in an ealier study [25]; for example, D scales with the ratio of B^2. In order to improve the initial higher order parameter estimates, isotopic ratios of the low-order parameters $A\zeta$, q, and F were also applied to the respective higher order parameters; thus q_J scales with the ratios of q and B. Initially, we assumed rotational corrections of $A\zeta$ and q to be the same in $v_8 = 1$ and 2; this holds rather often to first order. We point out that there are vibrational factors of these parameters which are different between $v_8 = 1$ and 2 in SPFIT. Vibrational changes ΔX of distortion parameters in $v_8 = 2$ were initially constrained to be two times those in $v_8 = 1$, which is frequently fulfilled to first order if l-dependent changes (of degenerate vibrational states) can be neglected.

We searched in each fitting round for a parameter whose floating in the fit improved the rms error of the fit the most. The only parameter tried out here that was not used in the fits of CH_3CN was f_{44}, which connects levels differing in $\Delta k = \Delta l = \pm 4$. It was retained in some $^{13}CH_3CN$ fits, but was omitted later because of its relatively large uncertainty. In the case of $v_8 = 1$ and 2 parameters, usually a parameter was floated with keeping the $v_8 = 1$ and 2 constraint before the effect of lifting this constraint was tested. Sometimes either procedure led to reinstating a constraint for a different parameter because of changes caused by correlation deemed to be too large. It appeared to be difficult, however, to avoid entirely much larger vibrational changes than suggested by the constraints. This applied in particular to ΔH_{KJ}, ΔH_{JK}, and ΔH_J. Attempts to impose constraints led to substantial increases in the rms errors that could not be compensated by other parameters.

Interestingly, it was possible to float one of the two $\Delta(A - B)$ values of $v_8 = 2$. Noting that $\Delta(A - B)$ of $v_8 = 2^2$ of $^{13}CH_3CN$ is slightly more than 2 MHz larger in magnitude than the one derived under the assumption of ΔA to be the same as the value of CH_3CN, we tried to impose this value. The rms error of the fit increased by ~10% and some parameters took less favorable values. Keeping this constraint and floating $\Delta(A - B)$ of $v_8 = 2^0$ instead, reduced the rms error to about the previous value and caused this $\Delta(A - B)$ value to decrease in magnitude by ~2 MHz with the remaining parameters fairly similar to those with $\Delta(A - B)$ of $v_8 = 2^2$ floated. Attempts to float both $\Delta(A - B)$ of $v_8 = 2$ decreased both in magnitude by ~8.5 MHz with uncertainties of about 5.5 MHz in the case of $^{13}CH_3CN$, whereas both increased by ~25 MHz with uncertainties of about 10 MHz in the case of $CH_3^{13}CN$. These findings suggest that the difference in $A - B$ between the two l substates of $v_8 = 2$ is well constrained, but the value of each is not quite yet. Therefore, we reverted to fitting only $\Delta(A - B)$ of $v_8 = 2^2$ and kept the one of $l = 0$ fixed at the estimated value.

The largest shifts by far caused by the HFS parameter $eQq\eta$ occur in the $\Delta F = 0$ HFS components of the $k = l = +1$ and

$k = l = -1$ transitions of $v_8 = 1$ and also in their $F = 1 - 0$ components of the respective $J = 2 - 1$ transitions. The shifts are essentially equal in magnitude and opposite in sign among the corresponding $k = l = +1$ and $k = l = -1$ HFS components.

The resulting spectroscopic parameters are listed in Table 1, Table 2, and Table 3 for $v_8 = 2$, 1, and for $v = 0$, respectively. The line, parameter, and fit files of both isotopomers are available as Supporting Information and have also been deposited in the CDMS as detailed in the Data Availability Statement.

5.5. Ground Vibrational States of $^{13}CH_3^{13}CN$, $^{13}CH_3C^{15}N$, and $CH_3^{13}C^{15}N$

The high enrichment of the $^{13}CH_3CN$ and $CH_3^{13}CN$ samples means that $^{13}CH_3^{13}CN$ is enriched in both samples to about 1.1% because of the natural $^{13}C/^{12}C$ ratio at the C atom that was not enriched. Moreover, $^{13}CH_3C^{15}N$ and $CH_3^{13}C^{15}N$ are enriched to about 0.38% in the $^{13}CH_3CN$ and $CH_3^{13}CN$ samples, respectively, because of the natural $^{15}N/^{14}N$ ratio. Therefore, our recordings covered some J of the respective isotopologs.

The $^{13}CH_3^{13}CN$ isotopolog was already studied quite extensively [23], albeit in natural isotopic composition. These measurements permitted transitions of several J to be identified between 249 and 1139 GHz with $K = 9$ in one transition. The present measurements accessed several J between 53 and 927 GHz and reached $K = 16$. The previous parameter set [23] was employed to fit the new data; calculations of the initial spectrum were taken from the CDMS. It was sufficient to fit H_J in addition to the parameters fit previously to achieve a satisfactory fit. The new spectroscopic parameters of $^{13}CH_3^{13}CN$ together with the earlier ones [23] and the resulting $^{13}CH_3C^{15}N$ and $CH_3^{13}C^{15}N$ are presented in Table 4.

Spectroscopic parameters of $^{13}CH_3C^{15}N$ and $CH_3^{13}C^{15}N$ were evaluated by assuming A_0 to be the same for isotopic species with substitutions of C or N atoms and by applying the $CH_3C^{15}N/CH_3CN$ parameter ratios and those involving $^{13}CH_3CN$ or $CH_3^{13}CN$ to the CH_3CN parameters for all others. Subsequently, B of each of these doubly substituted species was fit to the data from ref. 26, which covered $J = 1 - 0$ to $4 - 3$. These earlier data were omitted in the final fits because of more accurate data at similar quantum numbers obtained in the course of the present study.

The frequency ranges covered for these isotopomers here are very similar to the ones for $^{13}CH_3^{13}CN$, even more so, as its B value is similar to the $CH_3^{13}C^{15}N$ one, leading to occasional blending of the lines. The highest K value in both line lists is 15. The parameters fit for these two doubly substituted isotopomers were the same as the ones fit presently for $^{13}CH_3^{13}CN$. The parameter values and their uncertainties, as far as the parameters were fit, are also given in Table 4. The line, parameter, and fit files of all three doubly substituted isotopologs are available as Supporting Information and have also been deposited in the CDMS as detailed in the Data Availability Statement.

6. DISCUSSION OF THE LABORATORY RESULTS

Perhaps the most interesting results of the present study from the standpoint of molecular physics are the precise en-

Table 1: Spectroscopic Parameters or Vibrational Changes (Δ) with Respect to the Ground Vibrational States[a] of $^{13}CH_3CN$ and $CH_3{}^{13}CN$ in $v_8 = 2$ from a Combined Fit of $v_8 \leq 2$ Data and Comparison with Previous Data[b].

	$^{13}CH_3CN$		$CH_3{}^{13}CN$	
Parameter	This work	Previous[b]	This work	Previous[b]
$\Delta E(8^{2^2} - 8^{2^0})$	22.928605 (33)	22.37	21.792148 (16)	21.91
$\Delta(A - B)$	-185.58	-187.4	-187.74	-187.4
ΔB	52.100413 (32)	52.4115	52.219257 (44)	51.856
$\Delta D_K \times 10^3$	-20.4^c		-20.4^c	
$\Delta D_{JK} \times 10^3$	1.36866 (292)		1.45386 (225)	
$\Delta D_J \times 10^6$	211.432 (7)		202.613 (25)	
$\Delta H_{KJ} \times 10^6$	0.970 (62)		2.487 (25)	
$\Delta H_{JK} \times 10^9$	13.10 (46)		12.76 (4)	
$E(8^{2^2})$	738.65472 (76)	738.19	723.1949 (65)	723.01
$\Delta(A - B)$	-260.705 (120)	-260.0	-255.946 (79)	-260.0
ΔB	52.849506 (25)	52.84335	52.263148 (32)	52.2833
$\Delta D_K \times 10^3$	-20.4^c		-20.4^c	
$\Delta D_{JK} \times 10^3$	1.70985 (96)		1.52119 (107)	
$\Delta D_J \times 10^6$	178.371 (15)		182.257 (22)	
$\Delta H_{KJ} \times 10^6$	-0.1013 (43)		-0.1991 (55)	
$\Delta H_{JK} \times 10^9$	-2.252 (113)		-4.829 (159)	
$\Delta H_J \times 10^{12}$	521.4 (20)		536.7 (26)	
ΔeQq	-0.0798 (30)^c		-0.0888 (33)^c	
$A\zeta$	138847.16 (17)	138858.	139827.80 (8)	139829.5
η_K	10.0455 (62)^d		10.3882 (285)^d	
η_J	0.375339 (3)		0.392547 (3)	
$\eta_{KK} \times 10^6$	$-678.^d$		$-683.^d$	
$\eta_{JK} \times 10^6$	-31.939 (22)^d		-33.259 (27)^d	
$\eta_{JJ} \times 10^6$	-2.2659 (23)^d		-2.2689 (42)^d	
$\eta_{JKK} \times 10^9$	2.20^d		2.22^d	
$\eta_{JJK} \times 10^9$	0.5475 (56)^d		0.6462 (70)^d	
q	16.70353 (18)	16.7382	18.17787 (9)	18.1412
$q_K \times 10^3$	-2.089 (12)^d		-2.698^d	
$q_J \times 10^6$	-64.550 (35)		-68.183 (34)	
$q_{JK} \times 10^9$	90.06 (94)^d		79.11 (94)^d	
$q_{JJ} \times 10^{12}$	161.2 (43)		259.4 (46)	
$F(8^{\pm 1}, 8^{2,\mp 2})$	52777.6 (27)	51647. (1303)	50584.5 (51)	54567. (744)
$F_K(8^{\pm 1}, 8^{2,\mp 2})$	$-6.$	$-6.$	$-6.$	$-6.$
$F_J(8^{\pm 1}, 8^{2,\mp 2})$	-0.35815 (43)	-0.359	-0.35460 (41)	-0.370
$F_{JJ}(8^{\pm 1}, 8^{2,\mp 2}) \times 10^6$	1.700 (74)	1.58	1.783 (115)	1.70
$F_2(8^{\pm 1}, 8^{2,0}) \times 10^3$	-52.58 (5)^e		-55.37 (102)^e	
$F_2(8^{\pm 1}, 8^{2,\pm 2}) \times 10^3$	-105.16 (10)^e		-110.74 (204)^e	
$F_{2,J}(8^{\pm 1}, 8^{2,0}) \times 10^6$	-0.88^e		-0.98^e	
$F_{2,J}(8^{\pm 1}, 8^{2,\pm 2}) \times 10^6$	-1.76^e		-1.96^e	
rms error	0.877	0.766	0.891	0.808

[a] All parameters in MHz units except $E(8^{2^2} - 8^{2^0})$ and $E(8^{2^2})$ in cm^{-1}; the rms errors of the fits are unitless. Vibrational changes ΔX are defined as $X_i - X_0$. Numbers in parentheses are one standard deviation in units of the least significant figures. Parameters without quoted uncertainties were estimated and kept fixed in the analyses. [b] Reference 25. [c] The corresponding $v_8 = 2$ and $v_8 = 1$ parameters of each isotopomer were constrained to a 2 : 1 ratio; see also Section 5.4. [d] The corresponding $v_8 = 2$ and $v_8 = 1$ parameters of each isotopomer were constrained to a 1 : 1 ratio; see also Section 5.4. [e] A 1 : 2 ratio was constrained for $F_2(8^{\pm 1}, 8^{2,0})$ and $F_2(8^{\pm 1}, 8^{2,\pm 2})$ and also for their distortion corrections $F_{2,J}$, as done earlier for CH$_3$CN[16, 24].

Table 2: Spectroscopic Parameters or Vibrational Changes (Δ) Thereof[a] of ^{13}CH$_3$CN and CH$_3$^{13}CN in $v_8 = 1$ from a Combined Fit of $v_8 \leq 2$ Data and Comparison with Previous Data[b].

Parameter	^{13}CH$_3$CN		CH$_3$^{13}CN	
	This work	Previous[b]	This work	Previous[b]
$E(8^1)$	364.76782 (35)	364.56	357.19	357.19
$\Delta(A - B)$	−115.03	−115.930	−114.75	−115.930
ΔB	26.687766 (32)	26.688102 (131)	26.405025 (35)	26.404860 (112)
$\Delta D_K \times 10^3$	−10.2[c]	−11.46	−10.2[c]	−11.46
$\Delta D_{JK} \times 10^3$	0.95016 (39)	0.9453 (26)	0.86956 (45)	0.8811 (24)
$\Delta D_J \times 10^6$	90.447 (12)	90.693 (41)	92.400 (14)	92.585 (52)
$\Delta H_K \times 10^6$	20.8	15.	20.8	15.
$\Delta H_{KJ} \times 10^6$	0.0331 (16)	0.033	0.0202 (17)	0.034
$\Delta H_{JK} \times 10^9$	1.844 (63)	2.44	1.647 (81)	2.54
$\Delta H_J \times 10^{12}$	252.7 (17)	278.6 (56)	270.7 (18)	307.3 (74)
$\Delta L_J \times 10^{15}$		−2.35		−2.54
ΔeQq	−0.0399 (15)[c]	−0.0387	−0.0444 (17)[c]	−0.0387
$eQq\eta$	0.1647 (39)	0.1519	0.1562 (54)	0.1519
$A\zeta$	138859.445 (37)	138857.97 (53)	139838.800 (37)	139839.99 (39)
η_K	10.0455 (62)[d]	10.347	10.3882 (285)[d]	10.420
η_J	0.371752 (4)	0.371764 (23)	0.389217 (4)	0.389261 (24)
$\eta_{KK} \times 10^6$	−678.[d]	−835.	−683.[d]	−840.
$\eta_{JK} \times 10^6$	−31.939 (22)[d]	−32.87 (40)	−33.259 (27)[d]	−32.42 (44)
$\eta_{JJ} \times 10^6$	−2.2659 (23)[d]	−2.1471 (49)	−2.2689 (42)[d]	−2.2750 (52)
$\eta_{JKK} \times 10^9$	2.20[d]	2.5	2.22[d]	2.6
$\eta_{JJK} \times 10^9$	0.5475 (56)[d]	0.425 (70)	0.6462 (70)[d]	0.542 (69)
q	16.80179 (10)	16.80442 (35)	18.21027 (10)	18.21258 (33)
$q_K \times 10^3$	−2.089 (12)[d]	−2.516	−2.698[d]	−2.726
$q_J \times 10^6$	−58.697 (40)	−58.745 (164)	−64.596 (36)	−64.581 (175)
$q_{JK} \times 10^9$	90.06 (94)[d]	85.4	79.11 (94)[d]	95.2
$q_{JJ} \times 10^{12}$	295.3 (54)	301.0 (218)	319.8 (47)	304.8 (252)
$F_2(0, 8^{\pm 1}) \times 10^3$	−56.298 (15)			

[a] All parameters in MHz units except $E(8^1)$ in cm^{-1}. Vibrational changes ΔX are defined as $X_i - X_0$. Numbers in parentheses are one standard deviation in units of the least significant figures. Parameters without quoted uncertainties were estimated and kept fixed in the analyses. [b] Reference 25. [c] The corresponding $v_8 = 2$ and $v_8 = 1$ parameters of each isotopomer were constrained to a 2 : 1 ratio; see also Section 5.4. [d] The corresponding $v_8 = 2$ and $v_8 = 1$ parameters of each isotopomer were constrained to a 1 : 1 ratio; see also Section 5.4.

Table 3: Ground-State Spectroscopic Parameters[a] (MHz) of $^{13}CH_3CN$ and $CH_3^{13}CN$ from a Combined Fit of $v_8 \leq 2$ Data and Comparison with Previous Data[b].

| Parameter | $^{13}CH_3CN$ | | $CH_3^{13}CN$ | |
	This work	Previous[b]	This work	Previous[b]
$(A - B)$	149165.60	149165.69	148904.56	148904.65
B	8933.309448 (16)	8933.309429 (28)	9194.350055 (17)	9194.349998 (27)
$D_K \times 10^3$	2827.9	2831.	2827.9	2831.
$D_{JK} \times 10^3$	168.24018 (47)	168.23971 (130)	176.67618 (48)	176.67395 (132)
$D_J \times 10^6$	3625.018 (13)	3624.947 (32)	3809.866 (14)	3809.737 (37)
$H_K \times 10^6$	156.	165.	156.	165.
$H_{KJ} \times 10^6$	5.7894 (30)	5.8030 (141)	6.0018 (28)	6.0045 (131)
$H_{JK} \times 10^9$	927.18 (13)	927.19 (86)	1018.47 (15)	1017.45 (86)
$H_J \times 10^{12}$	−230.7 (44)	−273.3 (49)	−206.5 (52)	−258.4 (61)
$L_{KKJ} \times 10^{12}$	−400.0 (65)	−431.	−416.1 (55)	−444.
$L_{JK} \times 10^{12}$	−47.35 (34)	−49.66 (266)	−52.38 (33)	−49.75 (236)
$L_{JJK} \times 10^{12}$	−6.896 (16)	−6.887 (128)	−7.764 (20)	−7.214 (141)
$L_J \times 10^{15}$	−8.17 (50)	−2.76	−9.20 (61)	−3.10
$P_{JK} \times 10^{15}$	0.46	0.51	0.51	0.55
$P_{JJK} \times 10^{18}$	48.	49.	54.	55.
eQq	−4.21804 (152)	−4.21830 (197)	−4.21860 (145)	−4.21828 (176)
$C_{bb} \times 10^3$	1.79	1.792	1.84	1.844
$(C_{aa} - C_{bb}) \times 10^3$	−1.12	−1.10	−1.17	−1.15

[a] Numbers in parentheses are one standard deviation in units of the least significant figures. Parameters without quoted uncertainties have been estimated from the main isotopic species and were kept fixed in the fits. [b] Reference 23; adjusted in that work to account for slight changes in the parameters of the main isotopolog from that work compared to those in ref. 24.

ergy difference determinations between $v_8 = 1$ and 2 of both $^{13}CH_3CN$ and $CH_3^{13}CN$, the difference between $v_8 = 0$ and 1 for $^{13}CH_3CN$, and the differences between $v_8 = 2$, $l = 0$ and ± 2 for both isotopomers. The last type of determination is more generally possible in theory for a degenerate overtone state, but the precision with which this may be achieved depends obviously on how close energies get that have $\Delta k = \Delta l = \pm 2$ and what the magnitude of q_{22} is.

As can be seen in Table 1, the $\Delta E(8^{2^2} - 8^{2^0})$ values agree quite well with the initial estimates, slightly less so in the $^{13}CH_3CN$ case. And both values are quite close to the value of the main isotopic species, which are compared with other low-order parameters in Table 5. As mentioned in our previous study on CH_3CN [16], this type of energy difference appears to be challenging for quantum chemical calculations. Therefore, the present values are additional reference values besides the ones given in ref. 16 and other values presumably available in the literature. Overall, isotopic changes in the low-order parameters in Table 5 are small, and these differences display diverse trends. It is gratifying to see that $A\zeta$ and q are very similar in $v_8 = 1$ and 2 for each of the ^{13}C isotopomers, even though the values differ somewhat from those of the main isotopic species. Table 5 also demonstrates that the HFS parameters eQq, ΔeQq, and eQq_2 of both isotopomers agree well with the respective values −4.223, −0.039, and 0.152 MHz of the main isotopic species [16]. These values may also be compared with −4.710, −0.102, and 0.393 MHz of the lighter HCN molecule [56].

Interactions between a degenerate bending state and its overtone or the ground vibrational state have been reported comparatively rarely to the best of our knowledge. Examples besides CH_3CN are the isoelectronic molecules CH_3CCH [57, 58, 59] and CH_3NC [60]. In the case of $^{13}CH_3CN$, our $E(8^1)$ value of 364.77 cm^{-1} is 0.21 cm^{-1} higher than the value from low-resolution IR measurements [52], a very good agreement considering that there is no sharp Q-branch in a perpendicular b-type IR band. Our $E(8^{2^0})$ value of 715.73 cm^{-1} is 0.09 cm^{-1} lower than the low-resolution IR value [52]. The present $E(8^{2^2})$ value of 738.65 cm^{-1} is about 0.46 cm^{-1} higher than our previous estimate (Table 1). Inspection of the $CH_3^{13}CN$ values reveals that $E(8^{2^2})$ is nearly 0.2 cm^{-1} higher than our previous estimate, and the derived $E(8^{2^0})$ value of 741.40 cm^{-1} is 0.30 cm^{-1} higher than the value from low-resolution IR measurements [52]. Since, however, $E(8^{2^2})$ was determined with respect to a fixed $E(8^1)$ value, this may mean the true $E(8^1)$ value is somewhat lower. On the other hand, we need to keep in mind that the energy determinations here depend on several parameters that needed to be kept fixed. Besides $E(8^1)$ of $CH_3^{13}CN$, these are foremost $\Delta(A - B)$ of $v_8 = 1$ and $v_8 = 2^0$ for both isotopomers and possibly also $A - B$ in the ground vibrational state. While the last values are challenging to be determined, the $\Delta(A - B)$ values can be obtained from high-resolution IR measurements of v_8 and $2v_8$ or the $2v_8 - v_8$ hot band. Furthermore, effects on the spectroscopic parameters may be caused by the neglect of perturbation in $v_8 = 2$ by higher vibrational

Table 4: Spectroscopic Parameters[a] (MHz) of Methyl Cyanide Doubly Substituted Species and Dimensionless Weighted Standard Deviation wrms.

| Parameter | $^{13}CH_3^{13}CN$ | | $^{13}CH_3C^{15}N$ | $CH_3^{13}C^{15}N$ |
	This work	Previous[b]		
$(A - B) \times 10^{-3}$	149.171692	149.171692	149.434530	149.181347
B	8927.281134 (45)	8927.281294 (155)	8659.892784 (38)	8919.231179 (43)
D_K	2.8257	2.8257	2.8257	2.8257
$D_{JK} \times 10^3$	167.4232 (12)	167.4204 (177)	160.0445 (12)	168.4062 (11)
$D_J \times 10^3$	3.627251 (32)	3.627152 (61)	3.380957 (37)	3.556858 (42)
$H_K \times 10^6$	51.	51.	51.	51.
$H_{KJ} \times 10^6$	5.7497 (61)	5.50 (42)	5.4037 (77)	5.6355 (76)
$H_{JK} \times 10^6$	0.91905 (25)	0.9159 (35)	0.85813 (36)	0.94615 (29)
$H_J \times 10^{12}$	−292.0 (65)	−298.	−227.3 (76)	−156.7 (95)
$L_{KKJ} \times 10^{12}$	−427.	−427.	−412.	−419.
$L_{JK} \times 10^{12}$	−47.3	−47.3	−45.3	−45.3
$L_{JJK} \times 10^{12}$	−6.7	−6.7	−6.122	−6.916
$L_J \times 10^{15}$	−1.800	−1.800	−1.007	−1.007
$P_{JK} \times 10^{18}$	450.	450.	477.	526.
$P_{JJK} \times 10^{18}$	48.0	48.0	40.1	50.0
eQq	−4.2218 (53)	−4.21319		
$C_{bb} \times 10^3$	1.73	1.73		
$(C_{aa} - C_{bb}) \times 10^3$	−1.24	−1.24		
wrms	0.810	0.635	0.848	0.805

[a] Numbers in parentheses are one standard deviation in units of the least significant figures. Parameters without quoted uncertainties have been estimated and were kept fixed in the fits; see Section 5.5. [b] Reference 23.

Table 5: Comparison of Low Order Spectroscopic Parameters[a] of CH$_3$CN, ^{13}CH$_3$CN, and CH$_3$^{13}CN.

Parameter	CH$_3$CN[b]	^{13}CH$_3$CN	CH$_3$^{13}CN
$(A - B)_0$	148900.0	149165.6	148904.6
B_0	9198.899	8933.309	9194.350
eQq	-4.223	-4.218	-4.219
$F_2(0, 8^{\pm1}) \times 10^3$	-70.9	-56.3	
$E(8^1)$	365.024	364.77	357.19[c]
$\Delta(A - B)(8^1)$	-115.9	-115.0^d	-114.8^d
$\Delta B(8^1)$	27.530	26.688	26.405
$A\zeta(8^1)$	138656.0	138859.4	139838.8
$q(8^1)$	17.798	16.80	18.21
ΔeQq	-0.039	-0.040	-0.044
$eQq\eta$	0.152	0.165	0.156
$F(8^{\pm1}, 8^{2,\mp2})$	53138.	52778.	50585.
$\Delta E(8^{2^2} - 8^{2^0})$	22.398	22.929	21.792
$\Delta(A - B)(8^{2^0})$	-187.5	-185.6^d	-187.7^d
$\Delta B(8^{2^0})$	54.058	52.100	52.219
$E(8^{2^2})$	739.148	738.65	723.2
$\Delta(A - B)(8^{2^2})$	-260.1	-260.7	-255.9
$\Delta B(8^{2^2})$	54.503	52.850	52.263
$\Delta A(8^{2^2})$	-205.61	-207.9	-203.7
$A\zeta(8^{2^2})$	138655.4	138847.	139828.
$q(8^2)$	17.730	16.70	18.18

[a] All parameters in units of MHz, except energies E in units of cm^{-1}. Parameters from present fits unless indicated otherwise. [b] Reference 16. [c] From low-resolution IR measurements [52]. [d] Derived assuming the isotopic ΔA values agree with the corresponding CH$_3$CN values.

states, which may still be non-negligible even though substantial amounts of higher-k data of $l = 0$ and -2 were weighted out.

The $v_8 = 2^2$ ΔA values of both isotopomers deviate by $\sim$2 MHz from the value -205.61 MHz of CH$_3$CN [16], with the ^{13}CH$_3$CN value being slightly larger in magnitude (-207.9 MHz) and the CH$_3$^{13}CN being slightly smaller (-203.7 MHz), see also Table 5. The corresponding ΔB values agree very well with the previous estimates [25], as can be seen in Table 1, whereas the $v_8 = 2^0$ ΔB values deviate by slightly more than 0.3 MHz, potentially indicating unaccounted perturbations in the $v_8 = 2^0$ data included in the fit. The ΔD_{JK} and ΔD_J values point in a similar direction as those of $v_8 = 2^2$ are much closer to being two times the $v_8 = 1$ values than those of $v_8 = 2^0$. Deviations are more pronounced in the ΔH values, but still show the $v_8 = 2^2$ data to be closer to two times the $v_8 = 1$ values than those of $v_8 = 2^0$. Most of the rotational corrections to $A\zeta$ and q were constrained to being the same in $v_8 = 1$ and $v_8 = 2$; unconstrained parameters display various degrees of deviations. However, we should keep in mind that even in the latest account on the main isotopic species [16] some parameters remain which do not exhibit the usual $v_8 = 1$ to $v_8 = 2$ ratios. The $F(8^{\pm1}, 8^{2,\mp2})$ values are now quite well determined, showing some deviations from the previous values. The ^{13}CH$_3$CN value is now only slightly smaller than the 53.14 GHz of CH$_3$CN [16], whereas the CH$_3$^{13}CN value was previously somewhat larger than the CH$_3$CN value and now considerably smaller. However, these values may change somewhat upon better accounting of the higher-K data of the $l = 0$ and -2 substates.

Little needs to be mentioned concerning the present $v_8 = 1$ and $v = 0$ values in comparison to previous data. The uncertainties improved, in some cases around a factor of 10, because of the increased data sets even though additional parameters were floated in the fits. Changes in the lower order parameters are small, as it should be, while changes in some higher order parameters are not so small, which is not so unusual either. The interaction parameter $F_2(0, 8^{\pm1})$ of ^{13}CH$_3$CN is -56.3 kHz compared to -70.9 kHz for CH$_3$CN. The value of the ^{13}C species may well be affected by the chosen values of $\Delta(A - B)$ and other fixed parameters. We also obtained greatly improved spectroscopic parameters for ^{13}CH$_3$^{13}CN along with extensive parameter sets for ^{13}CH$_3$C^{15}N and CH$_3$^{13}C^{15}N.

7. ASTRONOMICAL RESULTS

We used the spectroscopic results obtained in Section 5.4 to search for rotational emission from within the $v_8 = 2$ vibrational state of the ^{13}C isotopomers of methyl cyanide toward the main hot molecular core of the Sgr B2(N) star-forming region. We employed the imaging spectral line survey ReMoCA carried out with ALMA between 84 and 114 GHz. Details about the observations and method of analysis of the survey can be found in Belloche et al. [61]. The spectra were analyzed under the assumption of local thermodynamic equilibrium with the Weeds software [62].
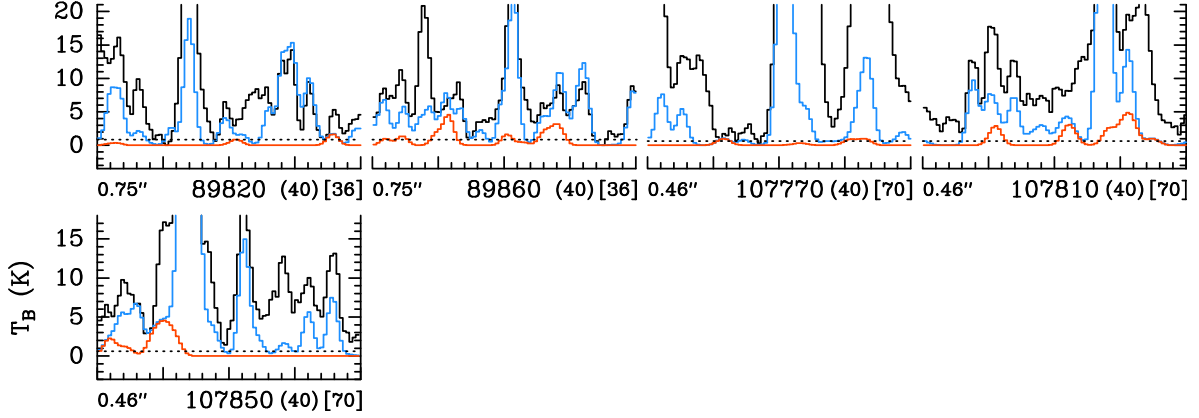
Figure 9: Transitions of $^{13}CH_3CN$ $v_8 = 2$ covered by the ReMoCA survey. The LTE synthetic spectrum of $^{13}CH_3CN$ $v_8 = 2$ is displayed in red and overlaid on the spectrum observed toward Sgr B2(N1S) shown in black. The blue synthetic spectrum contains the contributions of all molecules identified in our survey so far, including $^{13}CH_3CN$ $v_8 = 2$. The values written below each panel correspond from left to right to the half-power beam width, the central frequency in MHz, the width in MHz of each panel in parentheses, and the continuum level in K of the baseline-subtracted spectra in brackets. The y-axis is labeled in brightness temperature units (K). The dotted line indicates the 3σ noise level.
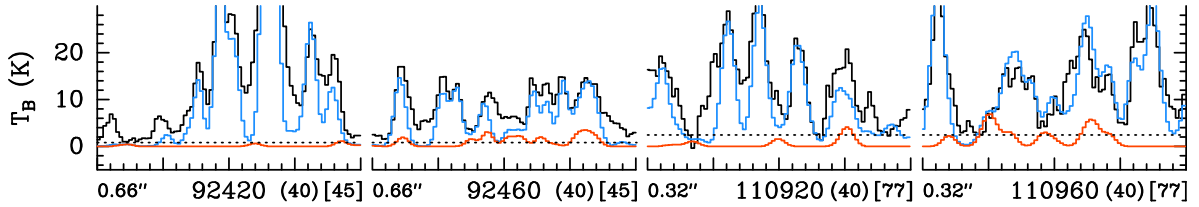

Figure 10: Same as Figure 9, but for $CH_3{}^{13}CN$ $v_8 = 2$.

Müller et al. [16] presented a detailed analysis of the emission of methyl cyanide in its vibrational ground state and several of its vibrationally excited states as well as its ^{13}C isotopologs in their vibrational ground state and in $v_8 = 1$, toward the position called Sgr B2(N1S), which is located within the main hot molecular core of Sgr B2(N). Using the same LTE parameters as in ref. 16, that is a column density of 1.4×10^{17} cm^{-2}, a temperature of 260 K, a line width of 6 km s^{-1}, and a systemic velocity of 61.8 km s^{-1}, we computed synthetic spectra for the ^{13}C isotopologs in $v_8 = 2$. This column density corresponds to a $^{12}C/^{13}C$ ratio of 21, which is typical for the Galactic center region[63, 21, 64, 65, 66].

The synthetic spectra of $^{13}CH_3CN$ $v_8 = 2$ and $CH_3{}^{13}CN$ $v_8 = 2$ are displayed in red and compared to the ReMoCA spectra shown in black in Figure 9 and Figure 10, respectively. The contributions of all molecules identified so far toward Sgr B2(N1S), including $^{13}CH_3CN$ $v_8 = 2$ and $CH_3{}^{13}CN$ $v_8 = 2$, is overlaid in blue. The synthetic spectra are consistent with the observed spectra with several lines above the 3σ noise limit, but no line of $^{13}CH_3CN$ $v_8 = 2$ and $CH_3{}^{13}CN$ $v_8 = 2$ is sufficiently free of contamination from other species to allow us to claim a robust identification of these states.

8. CONCLUSION

We employed methyl cyanide samples enriched in $^{13}CH_3CN$ and $CH_3{}^{13}CN$ to study their $v_8 = 2$ excited states extensively and to extend $v_8 = 1$ and 0 data sets. Perturbations sampled

the energy differences of the $l = 0$ and $l = \pm 2$ substates of $v_8 = 2$, the energy of $v_8 = 2$, and in the case of $^{13}CH_3CN$ the energy of $v_8 = 1$, thus improving our knowledge on the molecular properties of methyl cyanide.

A search for lines pertaining to $v_8 = 2$ of $^{13}CH_3CN$ and $CH_3{}^{13}CN$ toward Sgr B2(N1S) suggests that some of these lines are above the 3σ limit, but contamination by other species prevents a secure identification. Nevertheless, the results indicate that transitions of such high vibrational states and in isotopic species may well be identifiable in warm and dense parts of star-forming regions.

We also improved the $^{13}CH_3{}^{13}CN$ data set and obtained extensive spectroscopic parameters of $^{13}CH_3C^{15}N$ and $CH_3{}^{13}C^{15}N$ that are accurate enough to search for these rare isotopomers in space, even though the chances of finding them may be quite small.

tem. This paper makes use of the following ALMA data: ADS/JAO.ALMA # 2016.1.00074.S. ALMA is a partnership of ESO (representing its member states), NSF (USA) and NINS (Japan), together with NRC (Canada), MOST and ASIAA (Taiwan), and KASI (Republic of Korea), in cooperation with the Republic of Chile. The Joint ALMA Observatory is operated by ESO, AUI/NRAO and NAOJ.

Data Availability Statement

The input and output files of SPFIT are provided as supplementary material. These files as well as auxiliary files have been deposited in the data section of the CDMS [67]. Calculations of rotational spectra will be available in the catalog section of the CDMS [68].

9. Supporting Information

The Supporting Information is available free of charge at https://pubs.acs.org/doi/10.1021/acsearthspace-chem.5c00353.

The line, parameter, and fit files (with extensions .lin, .par, and .fit) are provided for all five isotopic species. The first file, numbered 001, explains the connection of the numbers with the respective isotopolog. All files are text files.

References

[1] P. M. Solomon, K. B. Jefferts, A. A. Penzias, R. W. Wilson, Detection of Millimeter Emission Lines from Interstellar Methyl Cyanide, Astrophys. J. Lett. 168 (1971) L107–L110. doi:10.1086/180794.

[2] See for example the Astrochymist Interstellar & Circumstellar Molecules page at http://www.astrochymist.org/astrochymist_ism.html; accessed 2025-11-10.

[3] S. Cazaux, A. G. G. M. Tielens, C. Ceccarelli, A. Castets, V. Wakelam, E. Caux, B. Parise, D. Teyssier, The Hot Core around the Low-mass Protostar IRAS 16293-2422: Scoundrels Rule!, Astrophys. J. 593 (1) (2003) L51–L55. doi:10.1086/378038.

[4] H. E. Matthews, T. J. Sears, Detection of the $J = 1 \rightarrow 0$ transition of CH_3CN., Astrophys. J. 267 (1983) L53–L57. doi:10.1086/184001.

[5] L. E. B. Johansson, C. Andersson, J. Ellder, P. Friberg, A. Hjalmarson, B. Hoglund, W. M. Irvine, H. Olofsson, G. Rydbeck, Spectral scan of Orion A and IRC +10216 from 72 to 91 GHz., Astron. Astrophys. 130 (1984) 227–256.

[6] R. Mauersberger, C. Henkel, C. M. Walmsley, L. J. Sage, T. Wiklind, Dense gas in nearby galaxies. V. Multilevel studies of CH_3CCH and CH_3CN., Astron. Astrophys. 247 (1991) 307.

[7] K. I. Öberg, V. V. Guzmán, K. Furuya, C. Qi, Y. Aikawa, S. M. Andrews, R. Loomis, D. J. Wilner, The comet-like composition of a protoplanetary disk as revealed by complex cyanides, Nature 520 (7546) (2015) 198–201. arXiv:1505.06347, doi:10.1038/nature14276.

[8] V. Thiel, A. Belloche, K. M. Menten, A. Giannetti, H. Wiesemeyer, B. Winkel, P. Gratier, H. S. P. Müller, D. Colombo, R. T. Garrod, Small-scale physical and chemical structure of diffuse and translucent molecular clouds along the line of sight to Sgr B2, Astron. Astrophys. 623 (2019) A68. arXiv:1901.03231, doi:10.1051/0004-6361/201834467.

[9] N. J. Livesey, M. D. Fromm, J. W. Waters, G. L. Manney, M. L. Santee, W. G. Read, Enhancements in lower stratospheric CH_3CN observed by the Upper Atmosphere Research Satellite Microwave Limb Sounder following boreal forest fires, J. Geophys. Res. 109 (D6) (2004) D06308. doi:10.1029/2003JD004055.

[10] I. J. Simpson, S. K. Akagi, B. Barletta, N. J. Blake, Y. Choi, G. S. Diskin, A. Fried, H. E. Fuelberg, S. Meinardi, F. S. Rowland, S. A. Vay, A. J. Weinheimer, P. O. Wennberg, P. Wiebring, A. Wisthaler, M. Yang, R. J. Yokelson, D. R. Blake, Boreal forest fire emissions in fresh Canadian smoke plumes: C_1-C_{10} volatile organic compounds (VOCs), CO_2, CO, NO_2, NO, HCN and CH_3CN, Atmos. Chem. Phys. 11 (13) (2011) 6445–6463. doi:10.5194/acp-11-6445-201110.5194/acpd-11-9515-2011.

[11] B. L. Ulich, E. K. Conklin, Detection of methyl cyanide in Comet Kohoutek, Nature 248 (5444) (1974) 121–122. doi:10.1038/248121a0.

[12] B. Bézard, A. Marten, G. Paubert, Detection of Acetonitrile on Titan, in: AAS/Division for Planetary Sciences Meeting Abstracts #25, Vol. 25 of AAS/Division for Planetary Sciences Meeting Abstracts, 1993, p. 25.09.

[13] P. F. Goldsmith, R. Krotkov, R. L. Snell, R. D. Brown, P. Godfrey, Vibrationally excited CH_3CN and HC_3N in Orion., Astrophys. J. 274 (1983) 184–194. doi:10.1086/161436.

[14] S. M. Fortman, J. P. McMillan, C. F. Neese, S. K. Randall, A. J. Remijan, T. L. Wilson, F. C. De Lucia, An analysis of a preliminary ALMA Orion KL spectrum via the use of complete experimental spectra from the laboratory, J. Mol. Spectrosc. 280 (2012) 11–20. doi:10.1016/j.jms.2012.08.002.

[15] A. Belloche, H. S. P. Müller, K. M. Menten, P. Schilke, C. Comito, Complex organic molecules in the interstellar medium: IRAM 30 m line survey of Sagittarius B2(N) and (M), Astron. Astrophys. 559 (2013) A47. arXiv:1308.5062, doi:10.1051/0004-6361/201321096.

[16] H. S. P. Müller, A. Belloche, F. Lewen, B. J. Drouin, K. Sung, R. T. Garrod, K. M. Menten, Toward a global model of the interactions in low-lying states of methyl cyanide: Rotational and rovibrational spectroscopy of the $v_4 = 1$ state and tentative interstellar detection of the $v_4 = v_8 = 1$ state in Sgr B2(N), J. Mol. Spectrosc. 378 (2021) 111449. `arXiv:2103.07389, doi:10.1016/j.jms.2021.111449`.

[17] S. E. Cummins, S. Green, P. Thaddeus, R. A. Linke, The kinetic temperature and density of the Sagittarius B2 molecular cloud from observations of methyl cyanide., Astrophys. J. 266 (1983) 331–338. `doi:10.1086/160782`.

[18] E. C. Sutton, G. A. Blake, C. R. Masson, T. G. Phillips, Molecular line survey of Orion A from 215 to 247 GHz., Astrophys. J. Suppl. Ser. 58 (1985) 341–378. `doi:10.1086/191045`.

[19] M. Gerin, F. Combes, G. Wlodarczak, T. Jacq, M. Guelin, P. Encrenaz, C. Laurent, Interstellar detection of deuterated methyl cyanide., Astron. Astrophys. 259 (1992) L35–L38.

[20] A. Nummelin, P. Bergman, Å. Hjalmarson, P. Friberg, W. M. Irvine, T. J. Millar, M. Ohishi, S. Saito, A Three-Position Spectral Line Survey of Sagittarius B2 between 218 and 263 GHz. I. The Observational Data, Astrophys. J. Suppl. Ser. 117 (2) (1998) 427–529. `doi:10.1086/313126`.

[21] A. Belloche, H. S. P. Müller, R. T. Garrod, K. M. Menten, Exploring molecular complexity with ALMA (EMoCA): Deuterated complex organic molecules in Sagittarius B2(N2), Astron. Astrophys. 587 (2016) A91. `arXiv:1511.05721, doi:10.1051/0004-6361/201527268`.

[22] H. Calcutt, J. K. Jørgensen, H. S. P. Müller, L. E. Kristensen, A. Coutens, T. L. Bourke, R. T. Garrod, M. V. Persson, M. H. D. van der Wiel, E. F. van Dishoeck, S. F. Wampfler, The ALMA-PILS survey: complex nitriles towards IRAS 16293-2422, Astron. Astrophys. 616 (2018) A90. `arXiv:1804.09210, doi:10.1051/0004-6361/201732289`.

[23] H. S. P. Müller, B. J. Drouin, J. C. Pearson, Rotational spectra of isotopic species of methyl cyanide, CH_3CN, in their ground vibrational states up to terahertz frequencies, Astron. Astrophys. 506 (3) (2009) 1487–1499. `arXiv:0910.3111, doi:10.1051/0004-6361/200912932`.

[24] H. S. P. Müller, L. R. Brown, B. J. Drouin, J. C. Pearson, I. Kleiner, R. L. Sams, K. Sung, M. H. Ordu, F. Lewen, Rotational spectroscopy as a tool to investigate interactions between vibrational polyads in symmetric top molecules: Low-lying states $v_8 \leq 2$ of methyl cyanide, CH_3CN, J. Mol. Spectrosc. 312 (2015) 22–37. `arXiv:1502.06867, doi:10.1016/j.jms.2015.02.009`.

[25] H. S. P. Müller, B. J. Drouin, J. C. Pearson, M. H. Ordu, N. Wehres, F. Lewen, Rotational spectra of isotopic species of methyl cyanide, CH_3CN, in their $v_8 = 1$ excited vibrational states, Astron. Astrophys. 586 (2016) A17. `arXiv:1512.05271, doi:10.1051/0004-6361/201527602`.

[26] H. S. Tam, J. A. Roberts, The vibration-rotation microwave spectrum of ^{13}C tagged acetonitrile in the region 17 to 75 GHz for the ground, $v_8 = 1$ and 2 vibrational states, J. Mol. Spectrosc. 134 (2) (1989) 281–289. `doi:10.1016/0022-2852(89)90314-7`.

[27] M. H. Ordu, H. S. P. Müller, A. Walters, M. Nuñez, F. Lewen, A. Belloche, K. M. Menten, S. Schlemmer, The quest for complex molecules in space: laboratory spectroscopy of n-butyl cyanide, $n-C_4H_9CN$, in the millimeter wave region and its astronomical search in Sagittarius B2(N), Astron. Astrophys. 541 (2012) A121. `arXiv:1204.2686, doi:10.1051/0004-6361/201118738`.

[28] M. A. Martin-Drumel, J. van Wijngaarden, O. Zingsheim, F. Lewen, M. E. Harding, S. Schlemmer, S. Thorwirth, Millimeter- and submillimeter-wave spectroscopy of disulfur dioxide, OSSO, J. Mol. Spectrosc. 307 (2015) 33–39. `doi:10.1016/j.jms.2014.11.007`.

[29] L.-H. Xu, R. M. Lees, G. T. Crabbe, J. A. Myshrall, H. S. P. Müller, C. P. Endres, O. Baum, F. Lewen, S. Schlemmer, K. M. Menten, B. E. Billinghurst, Terahertz and far-infrared synchrotron spectroscopy and global modeling of methyl mercaptan, $CH_3{}^{32}SH$, J. Chem. Phys. 137 (10) (2012) 104313. `doi:10.1063/1.4745792`.

[30] B. J. Drouin, F. W. Maiwald, J. C. Pearson, Application of cascaded frequency multiplication to molecular spectroscopy, Rev. Sci. Instr. 76 (9) (2005) 093113. `doi:10.1063/1.2042687`.

[31] J. Gadhi, A. Lahrouni, J. Legrand, J. Demaison, Dipole moment of CH_3CN, J. Chim. Phys. Phys.-Chim. Biol. 92 (1995) 1984–1992. `doi:10.1051/jcp/1995921984`.

[32] R. Anttila, V. M. Horneman, M. Koivusaari, R. Paso, Ground State Constants A_0, D_0^K and H_0^K of CH_3CN, J. Mol. Spectrosc. 157 (1) (1993) 198–207. `doi:10.1006/jmsp.1993.1016`.

[33] A. D. Becke, Density-functional thermochemistry. III. The role of exact exchange, J. Chem. Phys. 98 (7) (1993) 5648–5652. `doi:10.1063/1.464913`.

[34] C. Lee, W. Yang, R. G. Parr, Development of the Colle-Salvetti correlation-energy formula into a functional of the electron density, Phys. Rev. B 37 (2) (1988) 785–789. `doi:10.1103/PhysRevB.37.785`.

[35] T. H. Dunning, Jr., Gaussian basis sets for use in correlated molecular calculations. I. The atoms boron through

neon and hydrogen, J. Chem. Phys. 90 (2) (1989) 1007–1023. `doi:10.1063/1.456153`.

[36] M. J. Frisch, G. W. Trucks, H. B. Schlegel, G. E. Scuseria, M. A. Robb, J. R. Cheeseman, J. A. Montgomery, Jr., T. Vreven, K. N. Kudin, et al., Gaussian 03, Revision B.04, Gaussian, Inc., Wallingford CT (2003).

[37] H. M. Pickett, The fitting and prediction of vibration-rotation spectra with spin interactions, J. Mol. Spectrosc. 148 (2) (1991) 371–377. `doi:10.1016/0022-2852(91)90393-0`.

[38] H. M. Pickett, Spin eigenfunctions and operators for the D_n groups, J. Mol. Spectrosc. 228 (2) (2004) 659–663. `doi:10.1016/j.jms.2004.05.012`.

[39] B. J. Drouin, H. S. P. Müller, Special issue dedicated to the pioneering work of Drs. Edward A. Cohen and Herbert M. Pickett on spectroscopy relevant to the Earth's atmosphere and astrophysics, J. Mol. Spectrosc. 251 (1-2) (2008) 1–3. `doi:10.1016/j.jms.2008.05.004`.

[40] J. C. Pearson, H. S. P. Müller, H. M. Pickett, E. A. Cohen, B. J. Drouin, Introduction to submillimeter, millimeter and microwave spectral line catalog, J. Quant. Spectrosc. Radiat. Transfer 111 (2010) 1614–1616. `doi:10.1016/j.jqsrt.2010.02.002`.

[41] H. E. Radford, C. V. Kurtz, Stark effect and hyperfine structure of HCN measured with an electric resonance maser spectrometer., J. Res. Natl. Bur. Stand. 74A (1970) 791–799.

[42] J. M. L. J. Reinartz, A. Dymanus, Molecular constants of OCS isotopes in the (01 ^{1}0) vibrational state measured by molecular-beam electric-resonance spectroscopy, Chem. Phys. Lett. 24 (3) (1974) 346–351. `doi:10.1016/0009-2614(74)85275-9`.

[43] A. M. Tolonen, M. Koivusaari, R. Paso, J. Schroderus, S. Alanko, R. Anttila, The Infrared Spectrum of Methyl Cyanide Between 850 and 1150 cm^{-1}: Analysis of the ν_4, ν_7, and $3\nu_8^1$ Bands with Resonances, J. Mol. Spectrosc. 160 (2) (1993) 554–565. `doi:10.1006/jmsp.1993.1201`.

[44] R. Paso, R. Anttila, M. Koivusaari, The Infrared Spectrum of Methyl Cyanide Between 1240 and 1650 cm^{-1}: The Coupled Band System ν_3, $\nu_6^{\pm1}$, and $(\nu_7 + \nu_8)^{\pm2}$, J. Mol. Spectrosc. 165 (2) (1994) 470–480. `doi:10.1006/jmsp.1994.1150`.

[45] S. E. Novick, A beginner's guide to Pickett's SPCAT/SPFIT, J. Mol. Spectrosc. 329 (2016) 1–7. `doi:10.1016/j.jms.2016.08.015`.

[46] B. J. Drouin, Practical uses of SPFIT, J. Mol. Spectrosc. 340 (2017) 1–15. `doi:10.1016/j.jms.2017.07.009`.

[47] CDMS Fitting Spectra page at https://cdms.astro.uni-koeln.de/classic/pickett; accessed 2025-11-10.

[48] H. S. P. Müller, S. Thorwirth, D. A. Roth, G. Winnewisser, The Cologne Database for Molecular Spectroscopy, CDMS, Astron. Astrophys. 370 (2001) L49–L52. `doi:10.1051/0004-6361:20010367`.

[49] H. S. P. Müller, F. Schlöder, J. Stutzki, G. Winnewisser, The Cologne Database for Molecular Spectroscopy, CDMS: a useful tool for astronomers and spectroscopists, J. Mol. Struct. 742 (1-3) (2005) 215–227. `doi:10.1016/j.molstruc.2005.01.027`.

[50] C. P. Endres, S. Schlemmer, P. Schilke, J. Stutzki, H. S. P. Müller, The Cologne Database for Molecular Spectroscopy, CDMS, in the Virtual Atomic and Molecular Data Centre, VAMDC, J. Mol. Spectrosc. 327 (2016) 95–104. `arXiv:1603.03264, doi:10.1016/j.jms.2016.03.005`.

[51] H. Tam, I. An, J. A. Roberts, Microwave spectra of the ^{13}C isotopic species of methyl cyanide for the ground and $v_8 = 1, 2$ vibrational levels in the frequency range 17-56 GHz, J. Mol. Spectrosc. 129 (1) (1988) 202–215. `doi:10.1016/0022-2852(88)90270-6`.

[52] J. L. Duncan, D. C. McKean, F. Tullini, G. D. Nivellini, J. Perez Peña, Methyl cyanide. Spectroscopic studies of isotopically substituted species, and the harmonic potential function, J. Mol. Spectrosc. 69 (1) (1978) 123–140. `doi:10.1016/0022-2852(78)90033-4`.

[53] J. C. Pearson, H. S. P. Müller, The Submillimeter Wave Spectrum of Isotopic Methyl Cyanide, Astrophys. J. 471 (1996) 1067. `doi:10.1086/178034`.

[54] D. Boucher, J. Burie, J. Demaison, A. Dubrulle, J. Legrand, B. Segard, High-resolution rotational spectrum of methyl cyanide, J. Mol. Spectrosc. 64 (2) (1977) 290–294. `doi:10.1016/0022-2852(77)90267-3`.

[55] S. G. Kukolich, Beam maser spectroscopy on $J = 1 \rightarrow 2$, $K = 1$, and $K = 0$ transitions in CH$_3$CN and CH$_3$^{13}CN, J. Chem. Phys. 76 (1) (1982) 97–101. `doi:10.1063/1.442694`.

[56] S. Thorwirth, H. S. P. Müller, F. Lewen, S. Brünken, V. Ahrens, G. Winnewisser, A Concise New Look at the *l*-Type Spectrum of H^{12}C^{14}N, Astrophys. J. 585 (2) (2003) L163–L165. `doi:10.1086/374327`.

[57] H. S. P. Müller, P. Pracna, V. M. Horneman, The $v_{10} = 1$ Level of Propyne, H$_3$C−C≡CH, and Its Interactions with $v_9 = 1$ and $v_{10} = 2$, J. Mol. Spectrosc. 216 (2) (2002) 397–407. `doi:10.1006/jmsp.2002.8661`.

[58] P. Pracna, H. S. P. Müller, S. Klee, V. M. Horneman, Interactions in symmetric top molecules between vibrational polyads: rotational and rovibrational spectroscopy of low-lying states of propyne, H$_3$C−C≡CH,

Mol. Phys. 102 (14) (2004) 1555–1568. `doi:10.1080/ 00268970410001725864`.

[59] P. Pracna, H. S. P. Müller, Š. Urban, V. M. Horneman, S. Klee, Interactions between vibrational polyads of propyne, $H_3C-C\equiv CH$: Rotational and rovibrational spectroscopy of the levels around 1000 cm^{-1}, J. Mol. Spectrosc. 256 (1) (2009) 152–162. `doi:10.1016/j.jms. 2009.04.003`.

[60] P. Pracna, J. Urban, O. Votava, Z. Meltzerová, Š. Urban, V. M. Horneman, Rotational and rovibrational spectroscopy of the $v_8 = 1$ and 2 vibrational states of CH_3NC, Mol. Phys. 109 (17-18) (2011) 2237–2243. `doi:10. 1080/00268976.2011.605775`.

[61] A. Belloche, R. T. Garrod, H. S. P. Müller, N. J. Morin, S. A. Willis, K. M. Menten, Re-exploring Molecular Complexity with ALMA: Insights into chemical differentiation from the molecular composition of hot cores in Sgr B2(N2), Astron. Astrophys. 698 (2025) A143. `arXiv: 2505.03262, doi:10.1051/0004-6361/202554411`.

[62] S. Maret, P. Hily-Blant, J. Pety, S. Bardeau, E. Reynier, Weeds: a CLASS extension for the analysis of millimeter and sub-millimeter spectral surveys, Astron. Astrophys. 526 (2011) A47. `arXiv:1012.1747, doi:10.1051/ 0004-6361/201015487`.

[63] H. S. P. Müller, A. Belloche, K. M. Menten, C. Comito, P. Schilke, Rotational spectroscopy of isotopic vinyl cyanide, H_2CCHCN, in the laboratory and in space, J. Mol. Spectrosc. 251 (1-2) (2008) 319–325. `arXiv:0806. 2098, doi:10.1016/j.jms.2008.03.016`.

[64] H. S. P. Müller, A. Belloche, L.-H. Xu, R. M. Lees, R. T. Garrod, A. Walters, J. van Wijngaarden, F. Lewen, S. Schlemmer, K. M. Menten, Exploring molecular complexity with ALMA (EMoCA): Alkanethiols and alkanols in Sagittarius B2(N2), Astron. Astrophys. 587 (2016) A92. `arXiv:1512.05301, doi:10.1051/0004-6361/ 201527470`.

[65] D. T. Halfen, N. J. Woolf, L. M. Ziurys, The ^{12}C/^{13}C Ratio in Sgr B2(N): Constraints for Galactic Chemical Evolution and Isotopic Chemistry, Astrophys. J. 845 (2) (2017) 158. `doi:10.3847/1538-4357/aa816b`.

[66] A. M. Jacob, K. M. Menten, H. Wiesemeyer, R. Güsten, F. Wyrowski, B. Klein, First detection of ^{13}CH in the interstellar medium, Astron. Astrophys. 640 (2020) A125. `arXiv:2007.01190, doi:10.1051/ 0004-6361/201937385`.

[67] The present CH_3CN data are available at https://cdms.astro.uni-koeln.de/classic/predictions/daten/CH3CN/ in different subfolders; accessed 2026-01-08.

[68] See https://cdms.astro.uni-koeln.de/classic/entries/; accessed 2026-01-08.